Title

PARD3 induces TAZ activation and cell growth by promoting LATS1 and PP1 interaction

Journal

EMBO Reports, 16(8)

ISSN

1469-221X

Authors

Lv, Xian-Bo

Liu, Chen-Ying

Wang, Zhen

et al.

Publication Date

2015-08-01

DOI

10.15252/embr.201439951

Peer reviewed

Published online: June 26, 2015

Scientific Report

TRANSPARENT PROCESS

EMBO reports

PARD3 induces TAZ activation and cell growth by promoting LATS1 and PP1 interaction

Xian-Bo Lv[1,2,3], Chen-Ying Liu[4], Zhen Wang[1,2,3], Yi-Ping Sun[1,2,3], Yue Xiong[1,2,5,*], Qun-Ying Lei[1,2,**] & Kun-Liang Guan[1,2,6,***]

Abstract

The Hippo pathway plays a major role in organ size control, and its dysregulation contributes to tumorigenesis. The major downstream effectors of the Hippo pathway are the YAP/TAZ transcription co-activators, which are phosphorylated and inhibited by the Hippo pathway kinase LATS1/2. Here, we report a novel mechanism of TAZ regulation by the tight junction protein PARD3. PARD3 promotes the interaction between PP1A and LATS1 to induce LATS1 dephosphorylation and inactivation, therefore leading to dephosphorylation and activation of TAZ. The cytoplasmic, but not the tight junction complex associated, PARD3 is responsible for TAZ regulation. Our study indicates a potential molecular basis for cell growth-promoting function of PARD3 by modulating the Hippo pathway signaling in response to cell contact and cell polarity signals.

Keywords Hippo pathway; PARD3; TAZ; tight junction
Subject Categories Cell Adhesion, Polarity & Cytoskeleton; Signal Transduction
DOI 10.15252/embr.201439951 | Received 4 December 2014 | Revised 18 May 2015 | Accepted 26 May 2015 | Published online 26 June 2015
EMBO Reports (2015) 16: 975–985

Introduction

The first Hippo pathway component Warts was discovered in *Drosophila* by genetic mosaic screens for growth regulators [1]. The same approach was used to discover several other components of Hippo pathway, including Hippo, Sav, and Mob. Yki, the downstream effector, was identified by yeast two-hybrid screen. The Hippo pathway is highly conserved in mammals, in both pathway components and functions in organ size control and tissue homeostasis [2]. Key components of Hippo pathway consist of a kinase cascade of MST1/2 (Hippo homologs) and LATS1/2 (Warts homologs), downstream transcription co-activator YAP/TAZ (Yki homologs), and the transcription factor TEADs (Sd homologs). Forming complex with activated Mob1, LATS1/2 are phosphorylated and activated by MST1/2, the active LATS1/2 phosphorylate and inhibit YAP/TAZ. LATS1/2-dependent phosphorylation retains YAP/TAZ in cytoplasm and promotes YAP/TAZ degradation. Therefore, phosphorylation provides an important mechanism for YAP regulation (inhibition). The dephosphorylated YAP/TAZ are localized in cell nucleus and function as transcription co-activators to induce gene expression. However, YAP/TAZ have no DNA binding domain. Several YAP/TAZ target transcription factors have been identified. Among them, the TEAD family transcription factors are the most important to mediate the growth stimulating function of YAP/TAZ [3].

PARD3 is a PDZ-domain-containing scaffold protein that forms a trimetric complex with PAR6 and atypical protein kinase C (aPKC) to regulate the initial cell polarity cues [4]. Localized to the tight junctions, the PAR complex plays a critical role in cell polarity. It is required for neuroblast and epithelial polarization during Drosophila embryogenesis, and regulates various modes of polarization during neuronal development, migration, and tight junction formation in vertebrates [5–9]. PARD3 contains several evolutionarily conserved regions (CRs). The N-terminal domain CR1 is important for apical localization and dimerization of PARD3; the central CR2 consists of three PDZ domains that can interact with proteins with PDZ binding motifs; the CR3 is responsible for the binding and inhibition of aPKC and the C-terminal coil–coil domain [10].

PARD3 has been implicated to act as an invasion and metastasis suppressor. Inhibiting PARD3 causes loss of cell polarity and induces breast tumorigenesis and metastasis [11,12]. However, there are other reports showing that PARD3 may function as an oncogene [13]. Therefore, PARD3 may have dual functions, either promotion or suppression, in tumorigenesis in a manner dependent

1 Key Laboratory of Metabolism and Molecular Medicine, Ministry of Education and Department of Biochemistry and Molecular Biology, Fudan University Shanghai Medical College, Shanghai, China
2 Molecular and Cell Biology Lab, Institutes of Biomedical Sciences, Fudan University, Shanghai, China
3 School of Life Science, Fudan University, Shanghai, China
4 Department of Colorectal and Anal Surgery, Shanghai Colorectal Cancer Research Center, Xinhua Hospital, School of Medicine, Shanghai Jiaotong University, Shanghai, China
5 Department of Biochemistry and Biophysics, Lineberger Comprehensive Cancer Center, University of North Carolina at Chapel Hill, Chapel Hill, NC, USA
6 Department of Pharmacology and Moores Cancer Center, University of California San Diego, La Jolla, CA, USA
*Corresponding author. Tel: +1 919 962 2142; E-mail: yxiong@mai.unc.edu
**Corresponding author. Tel: +86 21 54237935; E-mail: qlei@fudan.edu.cn
***Corresponding author. Tel: +1 858 822 7945; E-mail: kuguan@ucsd.edu

on cancer types. In this report, we show that PARD3 activates YAP/TAZ to promote cell growth.

Results and Discussion

PARD3 stimulates YAP/TAZ dephosphorylation

In order to investigate TAZ regulation, we performed TAZ affinity purification and mass spectrometry (MS) and identified multiple putative TAZ-interacting proteins [3]. Notably, many polarity proteins and tight junction proteins were identified as TAZ-interacting proteins, results consistent with previous reports [14,15]. We then tested whether these putative interacting proteins regulated TAZ. Interestingly, overexpression of PARD3 reduced the phosphorylation of TAZ at Ser89 (Fig 1A), which is important for TAZ cytoplasmic localization and inhibition [16], while expression of other tight junction proteins had no significant effect on TAZ phosphorylation (Fig EV1A and B), suggesting that PARD3 has a unique function in TAZ regulation. YAP is a TAZ homolog and similarly regulated by the Hippo pathway. We found that PARD3 expression also reduced YAP2 (a splicing form of YAP) phosphorylation at Ser127 (Fig 1B), which is important for YAP cytoplasmic localization. These data suggest that PARD3 activates YAP/TAZ by reducing phosphorylation.

PARD3 forms a polarity complex with PAR6 and the atypical protein kinase C (aPKC). Both PAR6 and aPKC play indispensable roles in the regulation of various cell polarization events [17]. We examined the role of PAR6 and aPKC in the regulation of TAZ and observed that expression of either PAR6 or aPKC had no effect on the phosphorylation of TAZ Ser89 (Fig EV1C and D). Next, we knocked down *PARD3* using two different short hairpin RNAs in the A375 melanotic melanoma cell line and the T-47D breast cancer cell line. The knockdown efficiency was confirmed by real-time PCR (Fig EV1E). At low cell density, *PARD3* knockdown increased endogenous TAZ phosphorylation at Ser89, while a similar *PARD3* knockdown had no effect on TAZ phosphorylation when A375 cells were cultured at high density (Fig 1C). Similar observations were made with endogenous YAP phosphorylation in response to *PARD3* knockdown in T-47D cell line (Fig 1D). These data support a role of endogenous PARD3 in YAP/TAZ regulation. Moreover, our data suggest a cell density-dependent effect of PARD3 in regulating YAP/TAZ phosphorylation.

Next, we examined the functional consequences of PARD3 on YAP/TAZ activity using a well-established GAL4-TEAD luciferase reporter, which is directly regulated by YAP/TAZ activation status [16]. As expected, co-expression of PARD3 with TAZ augmented the GAL4-TEAD luciferase reporter activity in comparison with TAZ expression alone (Fig 1E). Together, the above observations indicate a physiological role of PARD3 in stimulating TAZ activity.

PARD3 promotes TAZ nuclear localization

Phosphorylation of TAZ at Ser89 creates a binding site for 14-3-3, which binds to and retains TAZ in cytoplasm. The above phosphorylation study suggests that PARD3 should inhibit the interaction between TAZ and 14-3-3. We performed co-immunoprecipitation (Co-IP) experiments with TAZ antibody and detected that overexpression of PARD3 inhibited the interaction between endogenous TAZ and 14-3-3 (Fig 2A). Consistently, cell fractionation experiments showed that TAZ protein levels were reduced in the cytoplasm and enriched in the nucleus in the presence of PARD3 (Fig 2B). Moreover, when *PARD3* was knocked down at low cell density, more TAZ protein was detected in the cytoplasmic fraction (Fig 2C). The immunofluorescence experiments further confirmed that knockdown of *PARD3* shifted TAZ to the cytoplasm (Fig 2D). These results are consistent with the phosphorylation data that PARD3 inhibits TAZ S89 phosphorylation. Phosphorylation of TAZ at residues Ser314 is required for binding of β-TrCP, a subunit of the SCF E3 ubiquitin ligase, and promotes TAZ ubiquitination and degradation [18]. We had also found that PARD3 expression reduced the interaction between TAZ and β-TrCP (Fig 2E). In addition, PARD3 enhanced the binding of TAZ and TEAD4 transcriptional factor (Fig 2F). Collectively, these data indicate that PARD3 promotes TAZ nuclear localization and association with TEAD4.

The aPKC binding region of PARD3 inhibits LATS1 by promoting its association with PP1A and dephosphorylation

We wanted to explore the mechanism how PARD3 inhibits TAZ, which is phosphorylated by LATS1/2 and dephosphorylated by PP1A [19]. We performed Co-IP experiments and detected that PARD3 neither reduced the interaction of TAZ with LATS1 nor increased the TAZ interaction with PP1A (Fig EV2A and B). Interestingly, PARD3 enhanced the interaction of endogenous PP1A and LATS1 (Fig 3A). Reciprocal Co-IP experiments also showed that PARD3 strengthened the association between PP1A and LATS1 (Fig EV2C). These results suggested that PARD3 may inhibit TAZ phosphorylation by inhibiting LATS1, which is activated by phosphorylation. Moreover, we also found that PARD3 interacted with PP1A and LATS1 (Fig EV2D and E), suggesting a possibility that PARD3 may act as a scaffold to facilitate the association between LATS1 and PP1A. To this end, we examined the effect of PP1A on LAST1 phosphorylation at Ser909, which is the site required for LATS1 kinase activation [20]. As expected, overexpression of PARD3 reduced the phosphorylation of endogenous LATS1 at Ser909 (Fig 3B). In the previous section (Fig 1C and D), we noted that the effect of PARD3 on YAP/TAZ phosphorylation was cell density dependent. Interestingly, an increased PP1/PARD3/LATS1 interaction was observed at low cell density in T-47D cells (Fig EV2F). Furthermore, we found that when *PARD3* was knocked down, the phosphorylation level of LATS1 on Ser909 was increased under low cell density, while no change was detected at high density under which LATS1 was already activated (Fig 3C). Expression of PARD3 is shown in Fig EV1E. In order to directly measure the kinase activity of LATS1, we performed an *in vitro* kinase assay using immunopurified LATS1 and bacterially purified His-TAZ protein as a substrate. We observed that PARD3 co-expression reduced LATS1 kinase activity toward TAZ (Fig 3D), demonstrating that LATS1 kinase activity was inhibited by PARD3 co-expression. The TAZ reporter assay also indicated that PARD3 suppressed the inhibitory effect of LATS1 on TAZ (Fig 3E).

Next, we examined whether LATS is required for PARD3 to modulate TAZ phosphorylation. For this purpose, we examined the *LATS1/2* KO (knockout) HEK293 cells that were created by CRISPR/Cas9 method. Consistent with our model, PARD3 expression had no

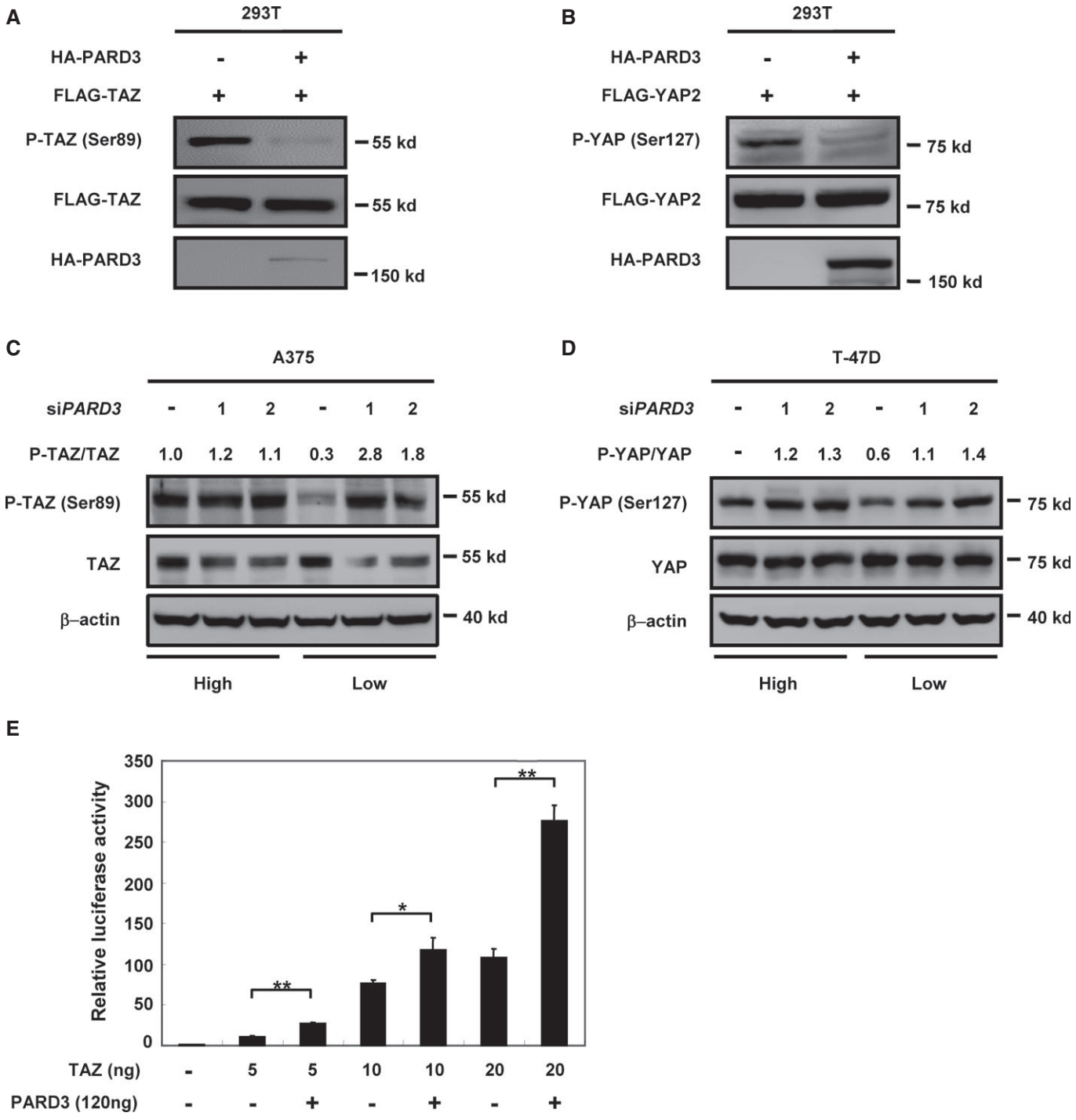

Figure 1. PARD3 decreases the phosphorylation and induces the activation of YAP/TAZ.

A PARD3 dephosphorylates TAZ at Ser89. HEK293T cells were transiently transfected with HA-PARD3 and FLAG-TAZ. Cells were harvested for Western blot analysis.

B PARD3 dephosphorylates YAP2 at Ser127. HEK293T cells were transiently transfected with the HA-PARD3 and FLAG-YAP2 as indicated; the cells were harvested for Western blot analysis.

C Knockdown of *PARD3* increases the phosphorylation of TAZ at Ser89 at low but not at high cell density. A375 cells were transfected with two different siRNAs for PARD3 under different cell densities (four times more cells were plated for high density than the low density), and cells were harvested for Western blot analysis.

D Knockdown of *PARD3* increases the phosphorylation of YAP at Ser127 at low cell density. T-47D cells were transiently transfected with the indicated siRNAs at different cell densities (4:1), and the cells were harvested for Western blot analysis as indicated.

E Co-expression of PARD3 enhances the activity of the transcriptional co-activator TAZ. Plasmids encoding the indicated proteins or empty PRK7 vector were cotransfected in HEK293T cells together with the TEAD reporter plasmids as indicated in Materials and Methods. The results are average ± SEM of three independent experiments. $*P < 0.05$, $**P < 0.01$.

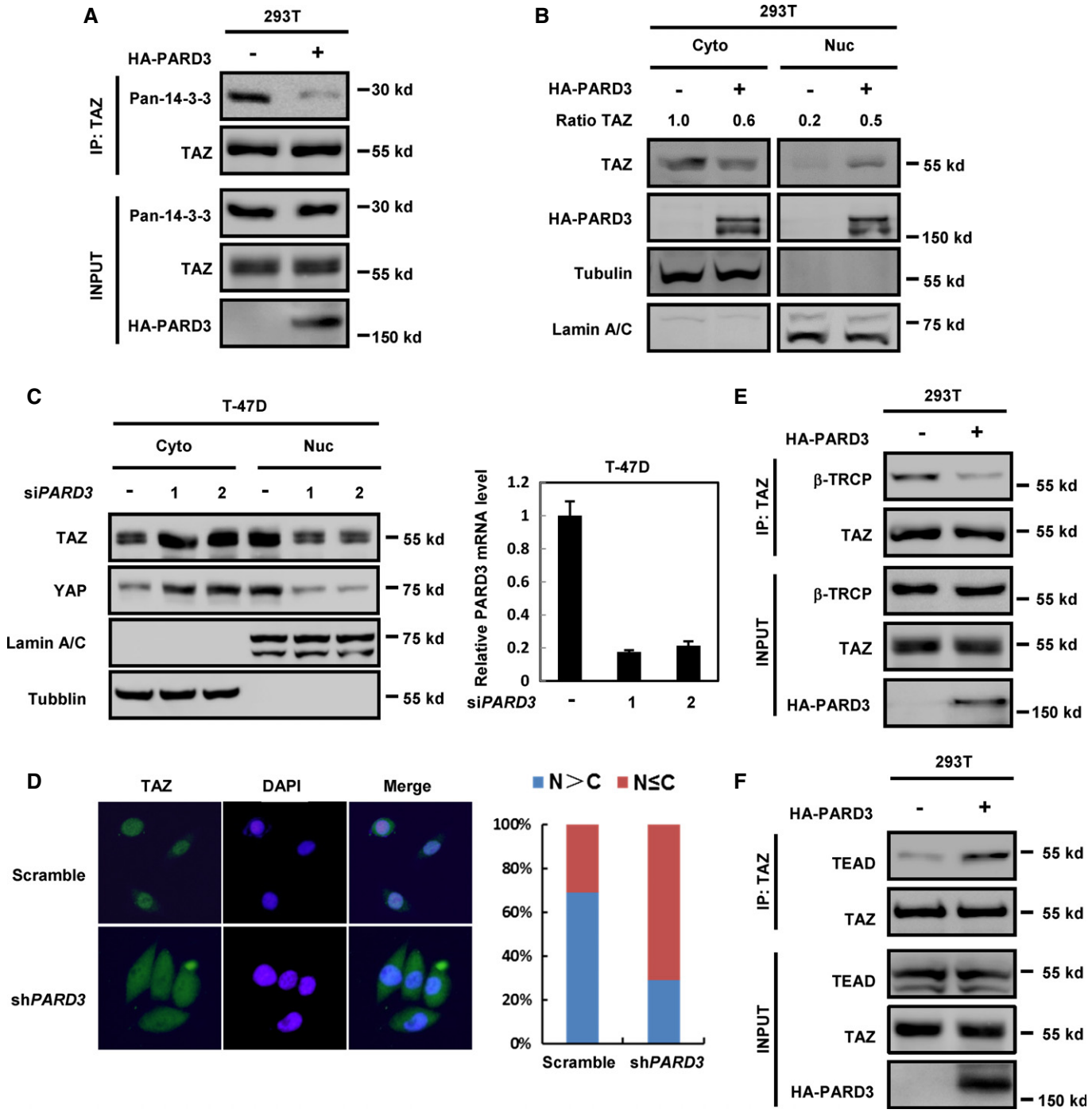

Figure 2. PARD3 promotes TAZ translocation into the nucleus.

A PARD3 decreases TAZ binding to 14-3-3. The indicated constructs were transfected into HEK293T cells. Immunoprecipitation with TAZ antibody was performed as indicated.

B PARD3 overexpression increases TAZ nuclear localization. Cell fractionation experiments were performed in PARD3-overexpressing T-47D cells as indicated for Western blot analysis.

C Left: *PARD3* knockdown decreases TAZ/YAP nuclear localization at low cell density. Cell fractionation experiments were performed in *PARD3*-knockdown T-47D cells as indicated. Right: Validation of siRNAs directed against PARD3. T-47D cells were transfected with the indicated siRNA. Forty-eight hours after transfection, the remaining expression level of PARD3 was determined using real-time PCR.

D *PARD3* knockdown promotes TAZ to shift to the cytoplasm. T-47D cells were stained with TAZ antibody, and DAPI stains cell nuclei.

E PARD3 decreases the interaction of endogenous TAZ with β-TrCP. 293T cells were transiently transfected with HA-PARD3. The samples were analyzed by Western blot after immunoprecipitation with TAZ antibody.

F PARD3 increases the interaction between endogenous TAZ and TEAD4. 293T cells were transiently transfected with HA-PARD3. The samples were analyzed by Western blot after immunoprecipitation with TAZ antibody.

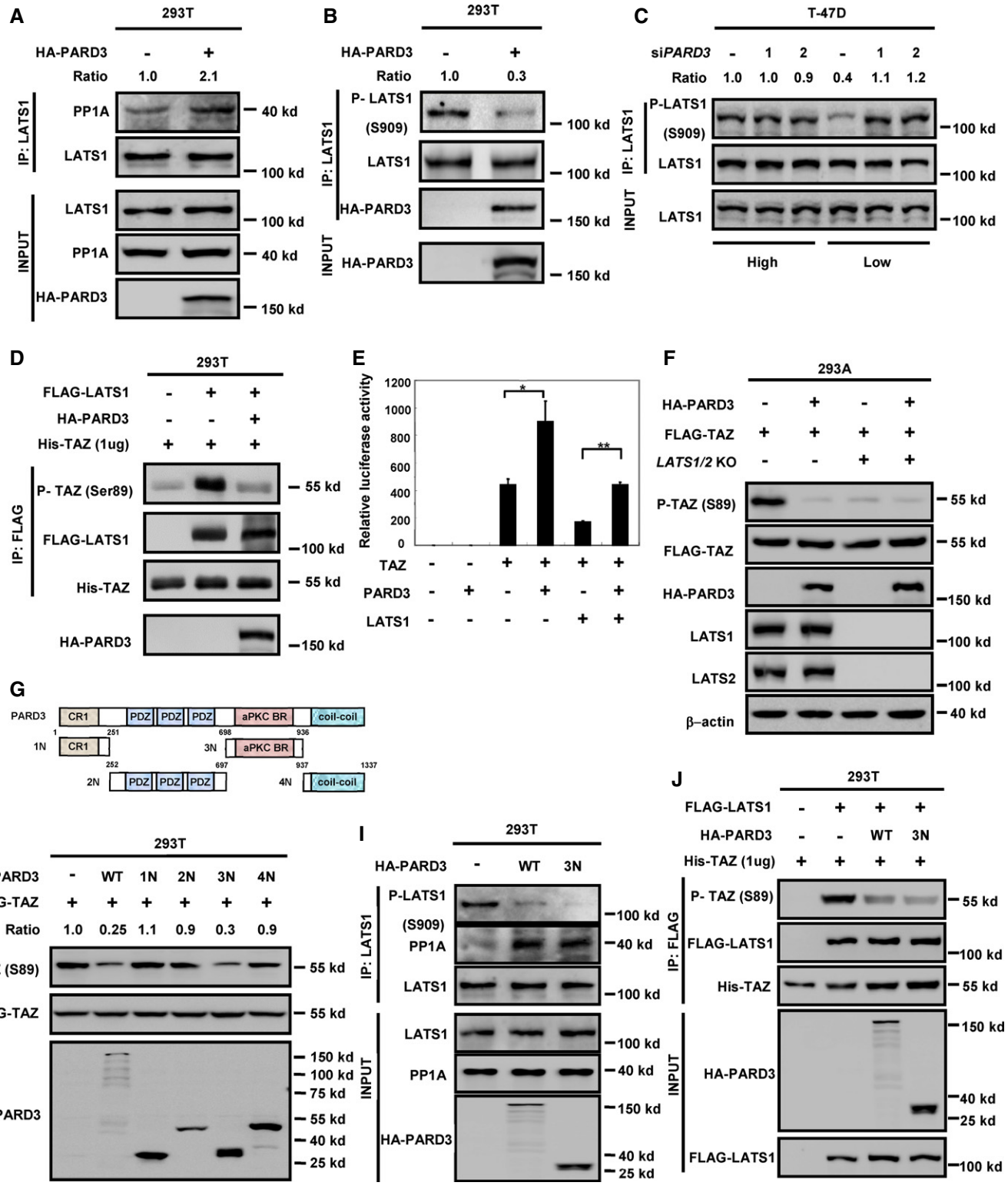

Figure 3.

effect on TAZ phosphorylation in the *LATS1/2* KO cells (Fig 3F), indicating that LATS1/2 are essential in TAZ regulation by PARD3. Furthermore, we observed that PARD3 still induced TAZ dephosphorylation in the wild-type LATS1, but not the LATS1 S909A mutant, rescued *LATS1/2* KO cells (Fig EV2G). Together, these results support a model that PARD3 inhibits LATS1 activity

Figure 3. The aPKC binding region of PARD3 dephosphorylates LATS1 at Ser909 to decrease the kinase activity of LATS1.

A PARD3 increases the binding of endogenous LATS1 and PP1A. The HA-PARD3 construct was transfected into HEK293T cells. Endogenous LATS1 was immunoprecipitated and subjected to Western blot analysis with indicated antibodies.

B PARD3 reduces the autophosphorylation of endogenous LATS1. HEK293T cells were transfected with the indicated plasmids. Western blot analysis was performed using a phospho-LATS1 (Ser909) antibody after immunoprecipitation with LATS1 antibody.

C Knockdown of *PARD3* increases the phosphorylation of LATS1 at Ser909 at low cell density. T-47D cells were transiently transfected with PARD3 siRNAs in different cell densities (4:1), immunoprecipitated with LATS1 antibody for Western blot analysis. The expression of PARD3 is shown in Fig EV1E.

D LATS1 activity is inhibited in the absence of PARD3. The indicated plasmids were transfected into HEK293T cells. LATS1 immunoprecipitated with FLAG antibody was subjected to *in vitro* kinase assay using His-TAZ purified from *E. coli* as a substrate. The products were analyzed by Western blotting as indicated.

E PARD3 increases the activity of TAZ with ectopically expressed LATS1. Plasmids encoding the indicated proteins were cotransfected in HEK293T cells together with the TEAD reporter plasmids. The luciferase assay showed that even if TAZ was inhibited by LATS1, PARD3 still activated TAZ. The results are average ± SEM of three independent experiments. $*P < 0.05$, $**P < 0.01$.

F PARD3 does not dephosphorylate TAZ in *LATS1/2* KO cells. The indicated constructs were transfected into *LATS1/2* KO 293A cells. The phosphorylation of TAZ was analyzed by Western blot as indicated.

G Schematic illustration of structure and deletion constructs of PARD3. Numbers refer to amino acid positions. aPKC-BR, aPKC binding region; CR1, conserved region 1; PDZ, PSD-95/Dlg/ZO-1.

H 3N construct (the aPKC binding region) is sufficient to dephosphorylate TAZ at Ser89. The indicated constructs were transiently transfected into HEK293T cells. Cell lysates were analyzed by Western blot as indicated.

I The 3N construct increases the interaction between endogenous LATS1 and PP1A. The indicated constructs were transfected into HEK293T cells, after immunoprecipitation with LATS1 antibody, and Western blot analysis was performed as indicated.

J LATS1 activity is inhibited in the absence of WT and 3N constructs of PARD3. LATS1 immunoprecipitated with FLAG antibody was subjected to *in vitro* kinase assay. The products were analyzed by Western blotting as indicated.

through increasing its interaction with PP1A, eventually leading to TAZ dephosphorylation and activation.

PARD3 consists of four domains: CR1 (1N), PDZ domains (2N), aPKC binding region (aPKC-BR, refer to 3N), and coiled-coil region (4N) (Fig 3G). Using deletion mutants, we showed that the aPKC-BR domain was sufficient to inhibit TAZ phosphorylation at Ser89, while the other domains had no effect (Fig 3H). We further performed co-immunoprecipitation experiments and found that overexpression of the aPKC-BR domain of PARD3 increased the binding of endogenous LATS1 with PP1A and reduced the phosphorylation of LATS1 at Ser909 (Fig 3I). The *in vitro* kinase assays also confirmed that ectopic expression of PARD3 aPKC-BR domain inhibited LATS1 kinase (Fig 3J). Collectively, these data indicate that the aPKC binding region of PARD3 is sufficient to inhibit LATS1 by promoting LATS1 and PP1A interaction.

Phosphorylation of Ser144/873 modulates PARD3 activity

Numerous studies have shown that PARD3 is regulated by phosphorylation. Phosphorylation of PARD3 at Ser144 and Ser873 by the serine/threonine kinase PAR1 disrupts epithelial apical–basal polarity and promotes multilumen cyst formation [21]. aPKC phosphorylates PARD3 at Ser827 to regulate epithelial tight junction [22], while RhoA stimulates PARD3 phosphorylation at Thr833 to disrupt PAR complex formation [23]. Moreover, PARD3 is also phosphorylated by Aura A at Ser962 to regulate its function in neuronal polarity [24]. We investigated whether these phosphorylation events might influence the activity of PARD3 in Hippo pathway regulation. PARD3 with mutations of the various phosphorylation sites were transfected into HEK293T cells, Western blot analysis revealed that the PARD3 S144A or S873A mutant was defective to inhibit TAZ phosphorylation when compared to the wild-type PARD3, while the other PARD3 mutants could still reduce TAZ phosphorylation (Figs 4A and EV3A). Ser144 and Ser873 in PARD3 are phosphorylated by PAR1, and phosphorylation of these residues releases PARD3 from the PAR complex at tight junctions into the cytoplasm [21]. To further test the function of PARD3 Ser144 and Ser873 phosphorylation, double mutants of phosphomimetic 2SD (S144D/S873D) and non-phosphorylatable 2SA (S144A/S873A) were generated. We first confirmed that wild type and 2SD mutant of PARD3 localized in both membrane and cytoplasm, while 2SA mutant mainly localized to plasma membrane (Fig EV3B). We found that PARD3 2SA mutant was inactive to decrease TAZ phosphorylation in the cotransfection experiments, while the PARD3 2SD could strongly inhibit TAZ phosphorylation (Fig 4B). In addition, ectopic expression of wild-type PARD3, but not the 2SA mutant, reduced the phosphorylation of endogenous LATS1 at Ser909 and increased the interaction between LATS1 and endogenous PP1A (Figs 4C and EV3C). We further determined LATS1 kinase activity and found that wild-type PARD3, but not the 2SA mutant, decreased LATS1 activity (Fig 4D).

It was reported that PAR1 inhibited kinase activity of Hippo in Drosophila [25]. We examined whether PAR1 also regulates the phosphorylation of TAZ. Overexpression of PAR1 decreased TAZ phosphorylation while silencing of *PAR1* increased the TAZ phosphorylation and inhibited the expression of TAZ target gene CTGF (Fig EV3D and E). However, PARD3 did not affect MST1/2 phosphorylation (Fig EV3F). These data indicate that phosphorylation at S144/S873 promotes PARD3 translocalization from tight junctions to cytosol and the cytoplasmic PARD3 promotes the interaction between LATS1 and PP1A, resulting in LATS1 dephosphorylation and inactivation. Notably, Huang *et al* [25] reported that overexpression of PAR1 inhibited Hpo-Thr195 phosphorylation and activity in fly cells; however, we detected that knockdown *PA*R1 reduced MST1/2 Thr180/183 phosphorylation (Fig EV3F). Our experiment was performed at high cell density, under which MST should be active. However, if we performed PAR1 knockdown at low cell density, the phosphorylation of MST1/2 at Thr180/183 was increased slightly (Fig EV3G). The above results indicate that the effect of PAR1 on MST Thr180/183 phosphorylation is cell density dependent. As PAR1 was reported to regulate several cell contact proteins, we speculate that effect of PAR1 knockdown on MST phosphorylation might be due to a consequence of altered cell contact, especially at high cell density.

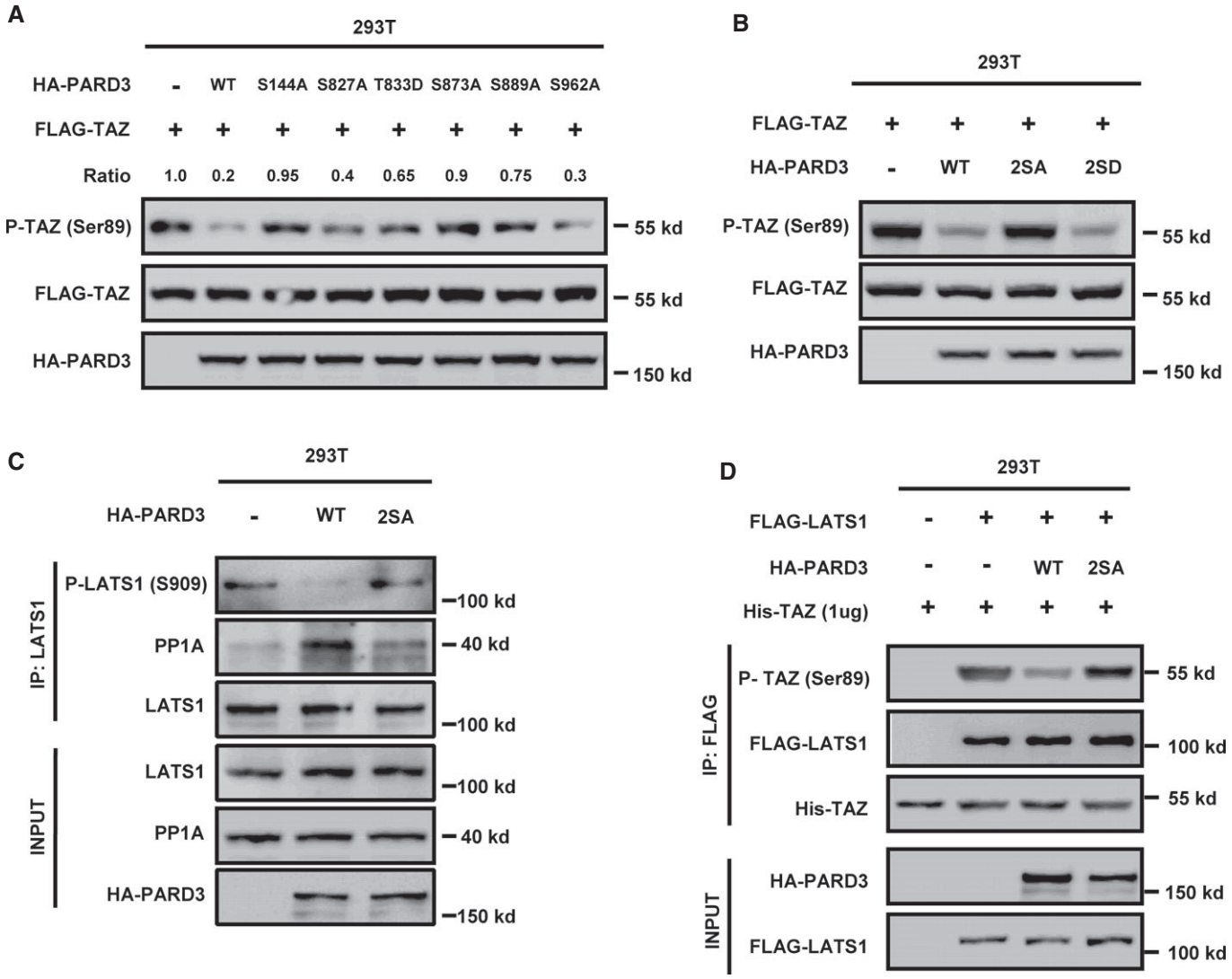

Figure 4. Phosphorylation of PARD3 at Ser144/Ser873 diminishes TAZ dephosphorylation.

A S144A and S873A mutations of PARD3 diminish TAZ dephosphorylation. PARD3 was reported to be regulated by phosphorylation. The indicated constructs that contain six point mutations of PARD3 were cotransfected with FLAG-TAZ into HEK293T. Western blot analysis was performed as indicated.

B Wild type and 2SD but not 2SA mutant of PARD3 decreases the phosphorylation of TAZ. The indicated constructs were transiently transfected into HEK293T cells. Western blot analysis was performed as indicated.

C The wild type but not 2SA mutant of PARD3 increases the binding of LATS1 and PP1A and decreases the phosphorylation of LATS1 at Ser909. The indicated constructs were transfected into HEK293T cells, and proteins were immunoprecipitated with LATS1 antibody. Cell lysates were analyzed by Western blot as indicated.

D LATS1 activity is not inhibited in the absence of 2SA mutant of PARD3. The indicated plasmids were transfected into HEK293T cells. LATS1 immunoprecipitated with FLAG antibody was subjected to *in vitro* kinase assay. The products were analyzed by Western blotting as indicated.

PARD3 regulates YAP/TAZ function in gene expression and cell growth

As a transcriptional co-activator, TAZ exerts its biological function by modulating target genes expression. We utilized a PARD3 siRNA oligo that was verified above and determined that knockdown of *PARD3* significantly reduced the mRNA level of TAZ target gene CTGF, FSTL1, PPPR1eB, PTSG2, and TAGLN when cells were cultured at low density (Fig 5A). However, *PARD3* knockdown did not significantly affect the expression of these TAZ target genes under high cell density. Interestingly, WT and 2SD mutant of PARD3 could rescue the expression of TAZ target genes in *PARD3* depletion cells, while the 2SA mutant did not (Fig EV4A). Moreover, *PARD3* knockdown in T-47D cells enhanced the ability of TAZ to reduce the expression of N-cadherin, a marker for mesenchymal cells, and to enhance E-cadherin, a marker for epithelial cells at low density (Figs 5B and EV4B). These results indicate that PARD3 modulates the expression of endogenous TAZ target genes.

YAP/TAZ positively promotes cell proliferation [16,26]. We examined whether PARD3 modulates cell growth. Knockdown of *PARD3* caused a significant reduction in cell growth in T-47D cells (Fig 5C). We also expressed the constitutively active TAZ-4SA, which cannot be phosphorylated and inhibited by LATS. As expected, the expression of TAZ-4SA promoted T-47D cell growth.

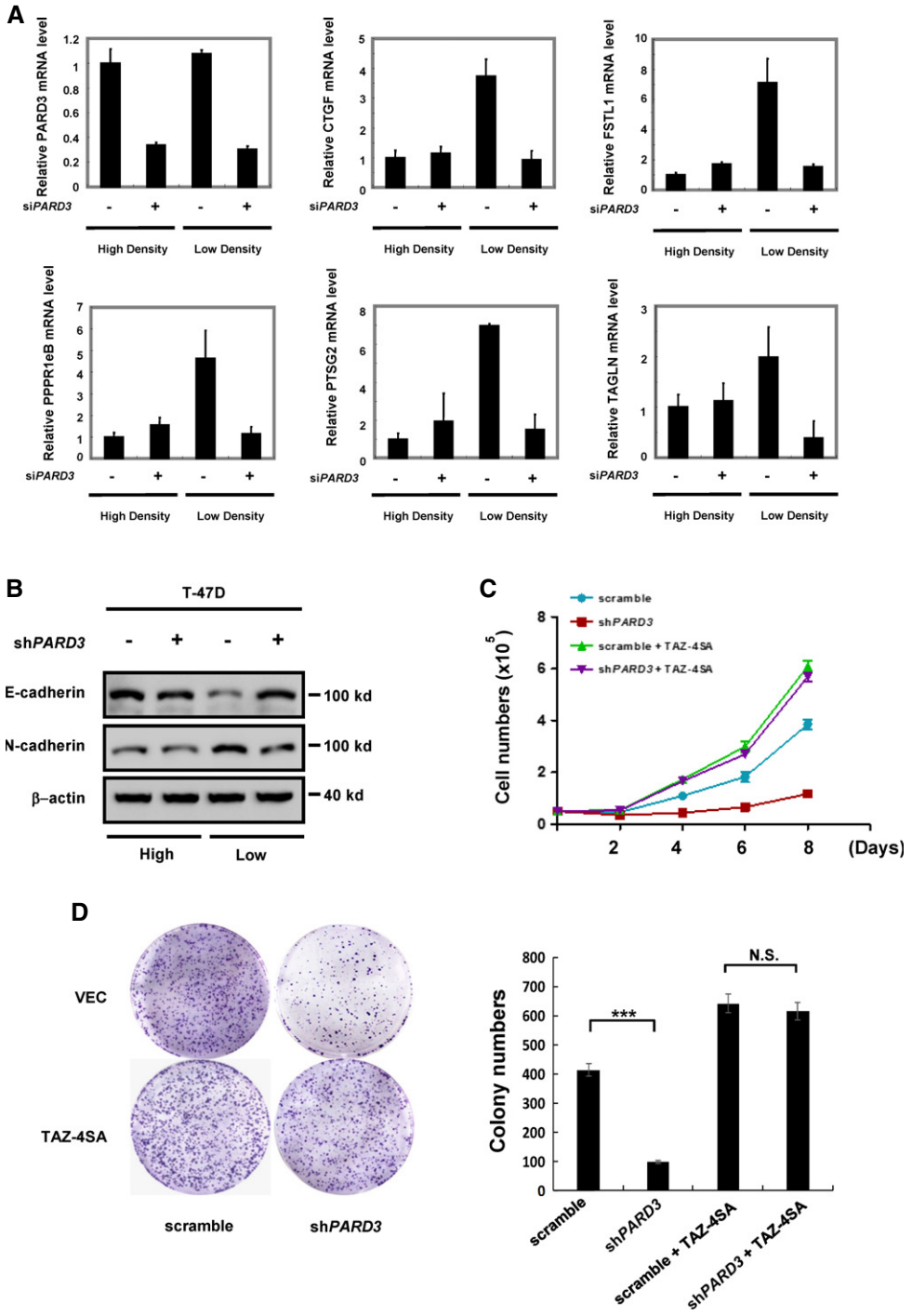

Figure 5. Knockdown of *PARD3* reduces the function of TAZ.

A Knockdown of *PARD3* leads to the decreased expression of the TAZ downstream targets *CTGF, FSTL1, PPPR1eB, PTSG2,* and *TAGLN* at low cell density (the ratio of high: low is 4:1). Forty-eight hours after transfection of the indicated siRNAs into T-47D cells, the target genes' expression levels and the knockdown of *PARD3* were analyzed using real-time PCR. The results are average ± SEM of three independent experiments.

B Knockdown of *PARD3* increases E-cadherin expression and decreases N-cadherin expression in T-47D cells at low cell density. The lysates were analyzed by Western blot, and all data are normalized to β-actin.

C TAZ-4SA expression blocks the inhibition of cell growth induced by *PARD3* knockdown. Growth curves of *PARD3*-knockdown T-47D cells overexpressing TAZ-4SA were determined. The results are average ± SEM of three independent experiments.

D TAZ-4SA expression blocks the inhibition of colony formation induced by *PARD3* knockdown. 5×10^3 *PARD3*-knockdown T-47D cells overexpressing TAZ-4SA were cultured in 6-well plates for 3 weeks before colonies were counted. Colonies were then visualized by crystal violet staining and counted. The results are average ± SEM of three independent experiments. N.S.: not significant, ***$P < 0.001$.

Importantly, cell growth of the TAZ-4SA-expressing cells was not sensitive to *PARD3* knockdown (Fig 5C). Similar results were observed when the constitutively active YAP2-5SA was tested (Fig EV4C). *PARD3* knockdown and YAP/TAZ expression were verified by real-time PCR and Western blot, respectively (Fig EV4D and E). Consistently, knocking down *TAZ* inhibited the growth of T-47D cells expressing PARD3 (Fig EV4F). These data are consistent with a role of PARD3 promoting cell growth by activating TAZ. Moreover, our observations suggest that PARD3 controls cell growth by modulating the phosphorylation status of YAP/TAZ. Finally, we investigated the role of PARD3 in anchorage-independent growth. Knockdown of *PARD3* inhibited colony formation of T-47D cells that could be overcome by TAZ-4SA expression (Fig 5D). Furthermore, WT and 2SD mutant of PARD3 could rescue colony formation in *PARD3*-knockdown cells, while 2SA did not (Fig EV4G). Together, our results support a model that PARD3 promotes cell growth by activating YAP/TAZ.

TAZ is a major functional output of the Hippo pathway, and it is regulated by dynamic reversible phosphorylation. In this report, we identified PARD3 as a potential activator of TAZ. It appears that the cytoplasmic PARD3, but not the tight junction associated, stimulates TAZ activity. YAP, the paralog of TAZ, is also regulated by PARD3 in a similar fashion. The scaffold protein PARD3 associates with PAR6 and atypical protein kinase C (aPKC) to regulate junction assembly and polarity [27]. Loss of these proteins or their dysregulation might result in disruption of polarity and carcinogenesis [28–30]. PARD3 localized at tight junctions between two neighboring epithelial cells when they contact each other. In scattered cells, PARD3 is in cytoplasm [31,32]. Our results indicate that PARD3 can activate TAZ by the following mechanism. At low cell density, the cytoplasmic PARD3 recruits the phosphatase PP1A to LATS1, thereby inducing LATS1 dephosphorylation and inactivation. When LATS is inhibited, TAZ phosphorylation is reduced and the dephosphorylated TAZ enters cell nucleus to bind TEAD and induce gene expression, resulting in stimulation of cell growth. At high density, PARD3 forms complex with PAR6 and aPKC and thus associates with the tight junction [4]. In addition, PARD3 can be regulated by the PAR1-dependent phosphorylation. PAR1 phosphorylates PARD3 at Ser144 and Ser873 and releases PARD3 from tight junction. The phosphorylated and cytoplasmic PARD3 then could activate TAZ. Our study also indicates that PP1A plays a crucial role in LATS1 dephosphorylation and activity regulation. Overexpression of PARD3 increases the interaction between PP1A and LATS1 as well as reduces LATS1 Ser909 phosphorylation and kinase activity. It has been reported that the tight junction protein AMOT inhibits YAP/TAZ by promoting their phosphorylation [33]. We propose that the tight junction might serve as a platform for Hippo pathway regulation in response to cell density and cell polarity. Our study suggests that tight junction proteins not only regulate cell polarity and cell–cell contact but also participate in cellular signaling.

Materials and Methods

Cell culture and transfection

HEK293T, A375, and T47D cells were cultured in Dulbecco's modified Eagle's medium (Invitrogen) supplemented with 10% fetal calf serum (MP Biomedicals) and 100 units/ml penicillin and streptomycin (Invitrogen). Cell transfection was performed using Lipofectamine 2000 (Invitrogen) or calcium phosphate method. Cells were harvested at 24 h post-transfection for protein analyses or luciferase activity assay. To establish stable *PARD3* knocking down cells, pMKO.1-sh*PARD3* retroviruses were generated and used to infect T-47D and A375 cells and stable pools were selected in puromycin (1 μg/ml)-containing media for 7 days. TAZ stable pool cells were seeded in 6-well plates with 5×10^4 cells/well in triplicate. Cell growth was counted every 2 days for 10 days.

Cell fractionation

HEK293T and T-47D cells were transiently transfected with HA-PARD3 constructs and siRNA targeting PARD3. Cells were lysed with subcellular fractionation buffer containing 250 mM sucrose, 20 mM HEPES, pH7.4, 10 mM KCl, 1.5 mM $MgCl_2$, 1 mM EDTA, 1 mM EGTA, 1 mM DTT, 1 mM PMSF, 25 mM NaF, and a mixture of protease inhibitors (Roche). Centrifuged out the nuclear pellet at 3,000 *g* for 10 min at 4°C, the cytoplasmic fraction was taken from the supernatant. The nuclear pellet was washed with the fractionation buffer and lysed with SDS buffer containing 50 mM Tris–HCl (pH 8.0), 150 mM NaCl, 0.1% SDS, 0.5% deoxycholate, 1% NP-40, 1 mM EDTA, 1 mM PMSF, 25 mM NaF, and cocktail protease inhibitors (Roche). Both fractions were analyzed by Western blot.

Immunofluorescence staining

Cells were fixed with 4% paraformaldehyde for 30 min and permeabilized with 0.1% Triton X-100 for 5 min at 4°C. After blocking in 0.5% BSA for 30 min, cells were incubated with the first antibody diluted in 0.5% BSA overnight. After washing with PBS for three times, cells were incubated with Alexa Fluor 488- or 594-conjugated secondary antibodies (1:1,000 dilution) for 1 h. Then, cells were subjected to fluorescence microscopy.

Luciferase assays

A mixture of activator plasmid (pGal4-TEAD), 5× upstream activating sequence (UAS)-luciferase reporter, and *Renilla* was cotransfected with the indicated plasmids (FLAG-TAZ, HA-PARD3, and control empty vectors) into HEK293T cells in a 24-well plate. Luciferase activity was measured after 24 h using a dual-luciferase reporter assay system (catalog no. E1960; Promega) by a luminometer (model TD-20/20). Transfection efficiency was normalized to thymidine kinase-driven Renilla luciferase activity.

Co-immunoprecipitation

HEK293T cells were transiently transfected using the calcium phosphate method, and the total amount of DNA was always adjusted with empty vectors. Lysed cells 24 h post-transfection with lysis buffer (50 mM Tris–HCl [pH 7.5], 150 mM NaCl, 1 mM EDTA, 0.3% NP-40, 50 mM NaF, 1.5 mM Na_3VO_4, protease inhibitor cocktail [Roche], 1 mM PMSF) for 30 min on ice and centrifuged at 12,000 *g* for 15 min at 4°C. The supernatant was incubated at 4°C for 3 h with the anti-FLAG (M2) antibody covalently coupled to

agarose beads (Sigma-Aldrich) or with the appropriate first antibody and 10 μl protein A agarose (Millipore). Before the addition of antibodies, a small aliquot of each supernatant was preserved and diluted with 5× SDS–PAGE sample buffer for later Western blot analysis (input). The beads were washed extensively with lysis buffer three times and centrifuged at 5,000 *g* for 5 min between each wash. Protein was eluted from beads with SDS sample buffer. Lysates were resolved on 8–10% SDS–polyacrylamide gels and transferred onto nitrocellulose (Bio-Rad) for Western blotting.

In vitro kinase assay

For the LATS1 kinase assays, HEK293T cells were transfected with the indicated constructs. Thirty-six hours post-transfection, cells were lysed with lysis buffer (50 mM HEPES [pH 7.5], 150 mM NaCl, 1 mM EDTA, 1% NP-40, 50 mM NaF, 1.5 mM Na_3VO_4, protease inhibitor cocktail [Roche], 1 mM dithiothreitol, 1 mM PMSF) and immunoprecipitated with anti-FLAG antibodies. The immunoprecipitates were washed three times with lysis buffer, followed by a single wash with wash buffer (40 mM HEPES, 200 mM NaCl) and a single wash with kinase assay buffer (30 mM HEPES, 50 mM potassium acetate, 5 mM $MgCl_2$). The immunoprecipitated LATS1 was subjected to a kinase assay in the presence of 500 μM cold ATP and 1 μg His-TAZ expressed and purified from Escherichia coli as the substrate. The reaction mixtures were incubated at 30°C for 30 min, terminated with sodium dodecyl sulfate (SDS) sample buffer. Phosphorylation was detected by Western blotting with the phospho-TAZ-specific antibody.

RNA isolation and real-time PCR

Total RNA was isolated from cultured cells using Trizol reagent (Invitrogen). cDNA was synthesized by reverse transcription using oligo (dT) (TransGen Biotech) as the primer and proceeded to real-time PCR with gene-specific primers in the presence of SYBR Premix Ex Taq (TaKaRa). The relative abundance of mRNA was calculated by normalization to β-actin mRNA.

Plasmids and antibodies

The constructs of TAZ, YAP2, LATS1, 14-3-3, β-TRCP, and PP1A were obtained as described previously. cDNA coding PARD3 was a gift from Dr.Tony Pawson. Point mutations and truncation of PARD3 were generated by site-directed mutagenesis and PCR. The short hairpin RNA sequence against PARD3 is GCCATCGACAAAT CTTATGAT.

Antibodies specific to FLAG (Sigma, F7425), HA (Santa Cruz, sc-7392), MYC (Huabio, H1208-1), GFP (Abmart, M20004) (CST#3195) YAP (Cell Signaling Technology, #4912), pYAP (S127) (CST#4911S), E-cadherin (CST#3195), N-cadherin (CST#4061), TEAD (BD Transduction Laboratories, 610922), LATS1 (Bethyl laboratory, A300-477A), pLATS1 (CST#9157), His (CST#2366), tubulin (NeoMarkers, #581P), LaminA/C (GenScript, A01455), and β-actin (GenScript, A00702) were purchased from commercial sources. Antibodies to TAZ and to phospho-TAZ (S89) were generated by immunizing rabbits with indicated antigen peptides at Shanghai Genomic Inc. Other materials and chemicals were obtained from commercial sources.

Colony formation assay

Colony formation assay was performed with T-47D breast cancer cell line. *PARD3* knocking down stable cells (5×10^3) were seeded on 6-well plates and maintained in DMEM supplemented with 10% fetal bovine serum for 2–3 weeks. Cells were fixed with 4% paraformaldehyde, and then, colonies were stained with 0.005% crystal violet.

Expanded View for this article is available online:
http://embor.embopress.org

Acknowledgements
We thank members of the Fudan Molecular and Cell Biology laboratory for discussion throughout this study. We also thank Biomedical Core Facility, Fudan University for technical support. This work was supported by MOST 973 (2015CB910401, 2011CB910601, 2012CB910103), NSFC (Grant No. 81430057, 81225016, 31271454), Shanghai Key basic research program (12JC1401100), and Shanghai Outstanding Academic Leader (Grant No. 13XD1400600) to Q.Y.L. This work was also supported by the Youth Science and Technology Leading Talent by MOST to Q.Y.L. This work was also supported and NIH grants (K.L.G. and Y.X.).

Author contributions
X-BL carried out most of the experiments and wrote the manuscript; C-YL contributed to some Western blot experiments; ZW helped with the RNAi and cell culture; Y-PS contributed to reagents' preparation and cell culture; YX, Q-YL, and K-LG supervised the entire project and wrote the manuscript.

Conflict of interest
The authors declare that they have no conflict of interest.

References

1. Justice RW, Zilian O, Woods DF, Noll M, Bryant PJ (1995) The Drosophila tumor suppressor gene warts encodes a homolog of human myotonic dystrophy kinase and is required for the control of cell shape and proliferation. *Genes Dev* 9: 534 – 546
2. Zhao B, Li L, Guan KL (2010) Hippo signaling at a glance. *J Cell Sci* 123: 4001 – 4006
3. Zhang H, Liu CY, Zha ZY, Zhao B, Yao J, Zhao S, Xiong Y, Lei QY, Guan KL (2009) TEAD transcription factors mediate the function of TAZ in cell growth and epithelial-mesenchymal transition. *J Biol Chem* 284: 13355 – 13362
4. Suzuki A, Ohno S (2006) The PAR-aPKC system: lessons in polarity. *J Cell Sci* 119: 979 – 987
5. Mertens AE, Rygiel TP, Olivo C, van der Kammen R, Collard JG (2005) The Rac activator Tiam1 controls tight junction biogenesis in keratinocytes through binding to and activation of the Par polarity complex. *J Cell Biol* 170: 1029 – 1037
6. Hirose T, Karasawa M, Sugitani Y, Fujisawa M, Akimoto K, Ohno S, Noda T (2006) PAR3 is essential for cyst-mediated epicardial development by establishing apical cortical domains. *Development* 133: 1389 – 1398
7. Goldstein B, Macara IG (2007) The PAR proteins: fundamental players in animal cell polarization. *Dev Cell* 13: 609 – 622
8. Pegtel DM, Ellenbroek SI, Mertens AE, van der Kammen RA, de Rooij J, Collard JG (2007) The Par-Tiam1 complex controls persistent migration

by stabilizing microtubule-dependent front-rear polarity. *Curr Biol* 17: 1623 – 1634

9. Costa MR, Wen G, Lepier A, Schroeder T, Gotz M (2008) Par-complex proteins promote proliferative progenitor divisions in the developing mouse cerebral cortex. *Development* 135: 11 – 22
10. Chen X, Macara IG (2005) Par-3 controls tight junction assembly through the Rac exchange factor Tiam1. *Nat Cell Biol* 7: 262 – 269
11. Xue B, Krishnamurthy K, Allred DC, Muthuswamy SK (2013) Loss of Par3 promotes breast cancer metastasis by compromising cell-cell cohesion. *Nat Cell Biol* 15: 189 – 200
12. McCaffrey LM, Montalbano J, Mihai C, Macara IG (2012) Loss of the Par3 polarity protein promotes breast tumorigenesis and metastasis. *Cancer Cell* 22: 601 – 614
13. Iden S, van Riel WE, Schafer R, Song JY, Hirose T, Ohno S, Collard JG (2012) Tumor type-dependent function of the par3 polarity protein in skin tumorigenesis. *Cancer Cell* 22: 389 – 403
14. Hauri S, Wepf A, van Drogen A, Varjosalo M, Tapon N, Aebersold R, Gstaiger M (2013) Interaction proteome of human Hippo signaling: modular control of the co-activator YAP1. *Mol Syst Biol* 9: 713
15. Couzens AL, Knight JD, Kean MJ, Teo G, Weiss A, Dunham WH, Lin ZY, Bagshaw RD, Sicheri F, Pawson T *et al* (2013) Protein interaction network of the mammalian Hippo pathway reveals mechanisms of kinase-phosphatase interactions. *Sci Signal* 6: rs15
16. Lei QY, Zhang H, Zhao B, Zha ZY, Bai F, Pei XH, Zhao S, Xiong Y, Guan KL (2008) TAZ promotes cell proliferation and epithelial-mesenchymal transition and is inhibited by the hippo pathway. *Mol Cell Biol* 28: 2426 – 2436
17. Ohno S (2001) Intercellular junctions and cellular polarity: the PAR-aPKC complex, a conserved core cassette playing fundamental roles in cell polarity. *Curr Opin Cell Biol* 13: 641 – 648
18. Liu CY, Zha ZY, Zhou X, Zhang H, Huang W, Zhao D, Li T, Chan SW, Lim CJ, Hong W *et al* (2010) The hippo tumor pathway promotes TAZ degradation by phosphorylating a phosphodegron and recruiting the SCF {beta}-TrCP E3 ligase. *J Biol Chem* 285: 37159 – 37169
19. Liu CY, Lv X, Li T, Xu Y, Zhou X, Zhao S, Xiong Y, Lei QY, Guan KL (2011) PP1 cooperates with ASPP2 to dephosphorylate and activate TAZ. *J Biol Chem* 286: 5558 – 5566
20. Chan EH, Nousiainen M, Chalamalasetty RB, Schafer A, Nigg EA, Sillje HH (2005) The Ste20-like kinase Mst2 activates the human large tumor suppressor kinase Lats1. *Oncogene* 24: 2076 – 2086
21. Yang Z, Xue B, Umitsu M, Ikura M, Muthuswamy SK, Neel BG (2012) The signaling adaptor GAB1 regulates cell polarity by acting as a PAR protein scaffold. *Mol Cell* 47: 469 – 483
22. Hirose T (2002) Involvement of ASIP_PAR-3 in the promotion of epithelial tight junction formation.pdf. *J Cell Sci* 115: 2485 – 2495
23. Nakayama M, Goto TM, Sugimoto M, Nishimura T, Shinagawa T, Ohno S, Amano M, Kaibuchi K (2008) Rho-kinase phosphorylates PAR-3 and disrupts PAR complex formation. *Dev Cell* 14: 205 – 215
24. Khazaei MR, Puschel AW (2009) Phosphorylation of the par polarity complex protein Par3 at serine 962 is mediated by aurora a and regulates its function in neuronal polarity. *J Biol Chem* 284: 33571 – 33579
25. Huang HL, Wang S, Yin MX, Dong L, Wang C, Wu W, Lu Y, Feng M, Dai C, Guo X *et al* (2013) Par-1 regulates tissue growth by influencing hippo phosphorylation status and hippo-salvador association. *PLoS Biol* 11: e1001620
26. Chan SW, Lim CJ, Guo K, Ng CP, Lee I, Hunziker W, Zeng Q, Hong W (2008) A role for TAZ in migration, invasion, and tumorigenesis of breast cancer cells. *Cancer Res* 68: 2592 – 2598
27. Assemat E, Bazellieres E, Pallesi-Pocachard E, Le Bivic A, Massey-Harroche D (2008) Polarity complex proteins. *Biochim Biophys Acta* 1778: 614 – 630
28. Feigin ME, Muthuswamy SK (2009) Polarity proteins regulate mammalian cell-cell junctions and cancer pathogenesis. *Curr Opin Cell Biol* 21: 694 – 700
29. McCaffrey LM, Macara IG (2011) Epithelial organization, cell polarity and tumorigenesis. *Trends Cell Biol* 21: 727 – 735
30. Royer C, Lu X (2011) Epithelial cell polarity: a major gatekeeper against cancer? *Cell Death Differ* 18: 1470 – 1477
31. Izumi Y, Hirose T, Tamai Y, Hirai S, Nagashima Y, Fujimoto T, Tabuse Y, Kemphues KJ, Ohno S (1998) An atypical PKC directly associates and colocalizes at the epithelial tight junction with ASIP, a mammalian homologue of Caenorhabditis elegans polarity protein PAR-3. *J Cell Biol* 143: 95 – 106
32. Horikoshi Y, Hamada S, Ohno S, Suetsugu S (2011) Phosphoinositide binding by par-3 involved in par-3 localization. *Cell Struct Funct* 36: 97 – 102
33. Zhao B, Li L, Lu Q, Wang LH, Liu CY, Lei Q, Guan KL (2011) Angiomotin is a novel Hippo pathway component that inhibits YAP oncoprotein. *Genes Dev* 25: 51 – 63